STEM CELLS TRANSLATIONAL MEDICINE®

TISSUE ENGINEERING AND REGENERATIVE MEDICINE

Anterior Cruciate Ligament Reconstruction in a Rabbit Model Using a Decellularized Allogenic Semitendinous Tendon Combined with Autologous Bone Marrow-Derived Mesenchymal Stem Cells

WEI LU,[a,*] JIAN XU,[a,*] SHIKUI DONG,[b,*] GUOMING XIE,[b,*] SHUANGHUI YANG,[c] XIAOQIAO HUANGFU,[b] XIAOXI LI,[b] YANG ZHANG,[b] PENG SHEN,[b] ZHAOWEN YAN,[d] HAIFENG LIU,[a] ZHENHAN DENG,[a] JINZHONG ZHAO[b]

[a]Department of Sports Medicine, the First Affiliated Hospital of Shenzhen University, Shenzhen Second People's Hospital, Shenzhen, People's Republic of China; [b]Department of Arthroscopic Surgery, Shanghai Jiao Tong University Affiliated Sixth People's Hospital, Shanghai, People's Republic of China; [c]Department of Hematology, Xiangya Hospital, Central South University, Changsha, People's Republic of China; [d]Department of Pathology, Shanghai Jiao Tong University School of Medicine, Shanghai, People's Republic of China

*Contributed equally

Correspondence: Zhenhan Deng, M.D., Ph.D., Department of Sports Medicine, the First Affiliated Hospital of Shenzhen University, Shenzhen Second People's Hospital, 3002 Sungang West Road, Shenzhen 518035, People's Republic of China. Tel: +86(0755)83366388; e-mail: dengzhenhan@email.szu.edu.cn or Jinzhong Zhao, M.D., Ph.D., Department of Arthroscopic Surgery, Shanghai Jiao Tong University Affiliated Sixth People's hospital, No. 600 Yishan Road, Shanghai 200233, People's Republic of China. Tel: +86(021) 64369181; e-mail: zhaojinzhong@vip.163.com

Received June 18, 2018; revised March 18, 2019; accepted for publication April 8, 2019; first published May 11, 2019.

http://dx.doi.org/10.1002/sctm.18-0132

Key Words. Bone marrow-derived mesenchymal stem cells • Anterior cruciate ligament • Decellularized allograft • Semitendinous tendon

ABSTRACT

As a regular adoptable material for anterior cruciate ligament (ACL) reconstruction, free tendon allograft exhibits unsatisfactory outcomes, such as retarded ligamentization and tendon–bone integration. The application of bone marrow-derived mesenchymal stem cells (BMSCs), as well as a decellularized free tendon allograft developed by our group, was proven to be effective in improving ACL reconstruction results. This study aimed to investigate the efficacy and feasibility of decellularized allogenic semitendinous tendon (ST) combined with autologous BMSCs used as a substitute to free tendon allograft in a rabbit model. This study finally shows that the decellularized allogenic ST combined with autologous BMSCs could significantly improve ACL reconstruction results compared with allograft. STEM CELLS TRANSLATIONAL MEDICINE *2019;8:971–982*

SIGNIFICANCE STATEMENT

Free tendon allograft exhibits unsatisfactory outcomes, such as retarded ligamentization and tendon–bone integration. The application of bone marrow-derived mesenchymal stem cells, as well as a decellularized free tendon allograft developed by the authors, was proven to be effective in improving anterior cruciate ligament reconstruction results.

INTRODUCTION

A total of 60,000 (20%) anterior cruciate ligament (ACL) reconstructions with allograft occur among 300,000 ACL reconstructions annually [1]. As ACL substitute materials, allograft has some outstanding advantages, including decreased donor site morbidity incidence and shortened operation time, when compared with autograft [2]. Meanwhile, multiple available types of allografts can be selected, and their sufficient supply can meet the needs in revision surgery or multiple ligament injuries [3]. Allografts are especially suitable for certain individuals, such as multiple ligament injuries or patients with donor site diseases. However, the clinical outcomes of ACL reconstruction with allograft are not always as satisfactory as those of autograft [1, 4]. The data from a series of basic research revealed that the poor outcome of allograft is related to slow graft ligamentization, delayed tendon–bone healing, and weak mechanical strength [2]. To some extent, most of these deficits are correlated with immunological rejection activity caused by extrinsic antigen [1, 2, 5–8]. Another potential threat to its wide use is the danger of disease transmission accompanied with allograft application. These diseases include clostridium, hepatitis B, hepatitis C, and acquired immunodeficiency syndrome [9, 10].

Scientists have used a number of methods to improve the outcome of ACL reconstruction surgery with free allogenic tendon graft. Among these methods, decellularization can diminish antigen components, improve physical characteristics, and ensure enhanced results [11, 12]. A decellularized allogenic free tendon graft with porous structure, low antigen, good compatibility, and sufficient mechanical strength was constructed by Whitlock et al., with the addition of peracetic acid (PAA); this graft can also effectively diminish deliberately infected pathogenic viruses [13].

Previous studies have demonstrated that bone marrow (BM)-derived mesenchymal stem cells (BMSCs) have prominent biological characteristics as a cell source for musculoskeletal disease, such as diseases affecting bone [14], cartilage [15], tendon [16], ligament [17], and tendon–bone healing [18]. Thus, if we performed ACL reconstruction combined with decellularized free tendon scaffold and autologous BMSCs in implantation, then the original acellular scaffold would exhibit vitality. Moreover, we hypothesized that this tissue-engineered complex may accelerate the process of ligamentization and strengthen tendon–bone integration. A rabbit model was used in this study.

METHODS

Autologous BMSC Harvest

In accordance with the procedures previously described by Soon et al. [19], the autologous primary BMSCs of New Zealand White (NZW) rabbits were extracted from the posterior iliac crest and cultivated with an untreated whole BM adherent culture technique for approximately 3 weeks before ACL reconstruction surgery. Rabbits were anesthetized with 30 mg/kg intravenous pentobarbital. A biopsy needle (2.0 mm diameter × 80 mm length) was inserted with rotational force into the unilateral iliac crest. Approximately 10 ml of BM aspirates was aspirated and collected with sterile polypropylene tubes, which contained 1,000 units/ml preservative-free heparin. An equal volume of phosphate-buffered saline (PBS) was added to the tubes. The BM and PBS were gently mixed, and the mixture was centrifuged for 10 minutes at 400*g* (Labofuge 400R, ThermoFisher, Osterode, Germany). The supernatant was discarded, and the remaining pellet was transferred into another sterile polypropylene tube, washed with PBS, and centrifuged twice. The pellets were resuspended and cultured in a T75 flask with growth medium consisting of 15 ml of Dulbecco's Modified Eagle's medium (DMEM; Cellgro, Manassas, VA) supplemented with 10% fetal bovine serum (FBS; Gibco, Carlsbad, CA) and antibiotics (100 U/ml penicillin and 100 μg/ml streptomycin; Gibco, Carlsbad, CA). The culture condition was set at 37°C, 5% CO_2, and 95% humidity. After 48 hours, nonadherent cells were discarded by changing the culture medium, and adherent cells were continuously cultured. The medium was changed every 3 days. When the culture dishes became nearly 90% confluent after approximately 10 days, the cells were detached with 0.25% trypsin-EDTA (Gibco, Carlsbad, CA) and serially subcultured. The cells in passage 3 were used in the cell application procedure.

Three Lineage Differentiation of BMSCs

The BMSCs in passage 3 underwent three lineage differentiation tests in vitro, namely, osteogenesis, chondrogenesis, and adipogenesis. The cells were seeded in a six-well plate at a density of 2.4×10^5 cells per well and cultured in growth medium until nearly 100% confluent. Appropriate inducing reagents were then added. In this test, commercialized differentiation kits were adopted following the manufacturer's guidelines. These kits included StemPro Osteogenesis Differentiation Kit (Gibco, Grand Island, NY), StemPro Chondrogenesis Differentiation Kit (Gibco, Grand Island, NY), and StemPro Adipogenesis Differentiation Kit (Gibco, Grand Island, NY). The cells cultured in growth medium served as control. Alizarin Red S (Sigma-Aldrich, St Louis, MO), Safranin O (Sigma-Aldrich, St. Louis, MO), and Oil Red O (Sigma-Aldrich, St. Louis, MO) were used for corresponding staining at the end of differentiation. The images were obtained with an inverted microscope (Leica, DFC295, Bensheim, Germany).

Lentivirus Vector Expressing Enhanced Green Fluorescent Protein Transfection

Lentivirus vector expressing enhanced green fluorescent protein (Lv-eGFP) was generated as previously described [20]. BMSCs in passage 2 were seeded at 6.5×10^5 onto a 10-cm dish and allowed to reach 80% confluence before transfection. The cells were transfected with Lv-eGFP at a multiplicity of infection of 50 pfu per cell for 12 hours and then continuously cultured in growth medium until complete confluence. A fluorescence microscope (Leica, DMI4000B, Wetzlar, Germany) was used to confirm successful labeling with eGFP. eGFP-positive cells were examined during the following tracing experiment.

Fresh Frozen and Decellularized Allogenic Semitendinous Tendon Preparation

A total of 172 fresh strips of semitendinous tendon (ST) grafts were obtained from adult NZW rabbits via homeochronous nonmusculoskeletal experiments. All the grafts were wrapped in saline-soaked gauze, placed in 15 ml falcon tubes and frozen immediately in −80°C and were used in the further experiment in 3 months.

A total of 92 fresh frozen ST grafts were decellularized to yield the decellularized ST grafts (pH = 7.2). The decellularization process was composed of two parts. The first part progressed according to the published protocol by Whitlock et al. [13]. This part generally includes the following steps: washing with distilled, deionized water (diH_2O) twice for 24 hours and digestion with 0.05% trypsin-EDTA for 1 hour. High-glucose DMEM with 10% FBS and 100 IU/ml penicillin/100 μg/ml streptomycin/0.25 μg/ml amphotericin B were used to halt digestion for 24 hours. The samples were washed with diH_2O for 24 hours and 1.5% PAA mixed with 2.0% Triton X-100 in diH_2O treatment for 4 hours. This step was followed by washing with diH_2O for 24 hours to multiply triple circles. The latter part was developed by our group, which was a procedure of neutralization with 5.0% $NaHCO_3$ dissolved in diH_2O for 8 hours, followed by washing with diH_2O twice for two 8 hours. The abovementioned processes were carried out in a shaker at 200 rpm and 37°C. Finally, the products were freeze dried and stored in sterile vessels at −80°C for further study. Aseptic technique was strictly obeyed throughout the whole procedure. Triton X-100 and $NaHCO_3$ were purchased from Sigma, and PAA was from Aladdin Industrial Corporation (China). Other chemicals were obtained from Gibco (Life Technologies, Invitrogen).

Double-Stranded ST Graft Preparation

Fresh frozen ST grafts were completely thawed at room temperature and then rehydrated in physiological saline for 20 minutes. For tissue-engineered grafts, the BMSCs in passage 3 were detached with 0.25% trypsin-EDTA (Gibco, Carlsbad, CA), and we halted digestion with the growth medium. The BMSCs were then centrifuged at 1,000 rpm for 5 minutes. The cell pellet was washed, centrifuged twice with sterile PBS, and resuspended with 4 ml of PBS in a sterile tube for subsequent experiments, in which each 1.0 ml of cell suspension contained 3.25×10^6 cells. Approximately 1.0 ml of BMSC suspension was superficially seeded and deeply injected into a decellularized tendon in line with the collagen fibers with a thin 25-gauge needle [21, 22].

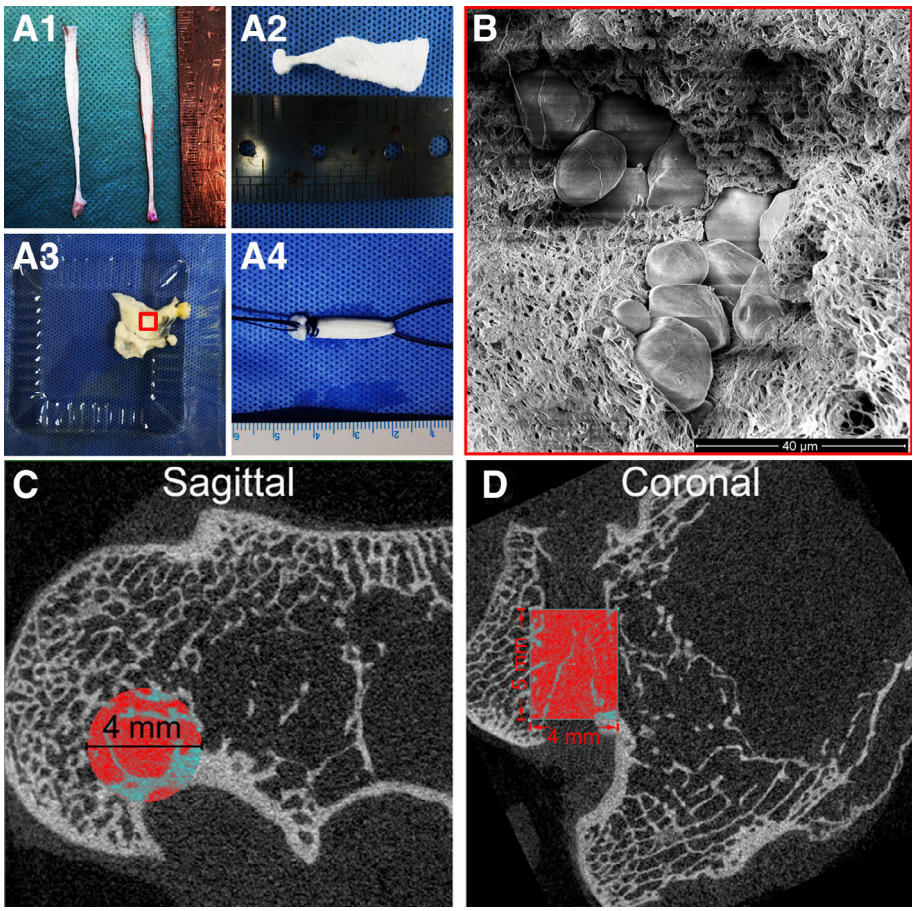

Figure 1. Gross images of the grafts and scanning electronic microscopy image of the prepared bone marrow-derived mesenchymal stem cells (BMSCs)/decellularized allograft graft, and schematic images of femoral condyle showing the region of interest (ROI) at micro-computed tomography analysis. **(A1):** Fresh frozen allogenic semitendinous tendon (ST) graft. **(A2):** Decellularized allogenic ST. **(A3):** The decellularized allogenic ST was being seeded with BMSCs. **(A4):** Well-prepared double bundle graft. **(B):** BMSCs seeded decellularized ST graft (×3000). **(C):** Marked the bottom of ROI at sagittal view. **(D):** Marked the length of ROI at coronal view.

After 20 minutes, the double bundle tissue-engineered graft was made following the same procedure (Fig. 1A).

First, the rehydrated fresh frozen ST or BMSC-seeded decellularized allogenic ST was folded accurately. The free ends were sutured together twice with Dexon 2-0 stitches by using locking whip stitches. Using this method, four strips of sutures at this end remained. The loop end was pulled through with one 2# ORTHOCORD suture (DePuy Mitek Raynham, MA). Approximately 5.0-cm-long sutures, which were used as retention sutures for fixation in a suspend manner, were kept at both ends. The end with four suture strips corresponded to the distal or tibia side, and the looped end with two suture strips corresponded to the proximal or femur side.

Animal Study

The protocol for use of the rabbits was reviewed and approved by the Animal Experiment Ethics Committee of Shenzhen Second People's Hospital, Shenzhen, Guangdong Province, China. This study was carried out in strict accordance with the Guidelines on the Care and Use of Laboratory Animals issued by the Chinese Council on Animal Research and the Guidelines of Animal Care.

A total of 86 skeletally mature male NZW rabbits of 8 months old weighing 3.0–3.5 kg at the time of surgery were included in the study. They were randomly divided into the fresh frozen allograft group (i.e., FFA group, in which ACL was reconstructed with fresh frozen decellularized allogenic ST) and the tissue engineered graft group (i.e., BMSC/decellularized allograft (DA) group, in which ACL was reconstructed with decellularized allogenic ST combined with BMSCs). The FFA group contained 40 rabbits, whereas the BMSC/DA group contained 46 rabbits, among which six rabbits were used for eGFP-labeled BMSC tracing test. Each animal received bilateral ACL reconstruction with the same kind of graft. Four observation time points were set, that is, weeks 2, 4, 8, and 12. Five rabbits in either group were sacrificed at each time point with both sides of the knee joints collected. The left knee (N = 5/group/time point) was subjected to biomechanics test and microcomputed tomography (micro-CT) analysis. The right knee was used for histology. Two rabbits with eGFP-labeled BMSC implantation were executed at each time point, that is, weeks 4, 8, and 12. In addition, the harvested samples were used for BMSC tracing examination. All the surgical procedures were accomplished by two experienced investigators.

All animals received bilateral ACL reconstruction in accordance with an established model [23]. After anesthesia, the initial ACL was surgically excised from its femur and tibia insertion under sterile conditions. Through the center of ACL footprints, the bone tunnels were drilled with a 2.0-mm-thick Kirschner wire, and the bone tunnels were angled 30°–45° to the long axis of the lower limb. In the BMSC/DA group, 1.0 ml of

BMSC suspension (3.25×10^6 cells) were injected into the femoral and tibia bone tunnels before graft implantation. In the FFA group, 1 ml of PBS was injected into the bone tunnels. The prepared double bundle graft was pulled into the bone tunnels through a 0.8-mm-diameter guide wire and sutured to the periosteum and the surrounding soft tissues overlaying the lateral femoral condyle or the medial tibial tuberosity, and then the graft was fixed in a suspend manner with double U-shape screws made of Kirschner wire to fix the sutures to the cortex [20]. After implantation, the capsule and skin were sutured discontinuously in layers.

After the surgery, the animals were allowed to reach full cage activity and received protective antibiotics via intramuscular injection and incision sterilization once a day for 3 days. All animals survived up to the observation time point, with no inflammation and other unhealthy events.

Histological Evaluation

After micro-CT scanning examination, the tendon–bone complex samples were prepared in accordance with a previously reported protocol [24]. This protocol included a series of regular procedures: 10% buffered formalin fixation, 10.0% ethylenediaminetetraacetic acid decalcification, graded dehydration in alcohol, transparent in chloroform, and paraffin embedding. The intra-articular graft samples were prepared without decalcification. Longitudinal 5 μm-thick sections were cut. The intra-articular sections were stained with H&E, and the intraosseous sections were stained by Masson trichrome (M-T) staining. The collagen fiber arrangement of the intra-articular graft samples was observed by polarized microscopy. The polarized and corresponding H&E images were captured via polarized light microscopy (Zeiss Axiolab, ZEISS, Germany). The other images were obtained by light microscopy (DM2500; Leica, Solms, Germany). The histology images were converted to gray scale and the level of collagen birefringence expression was quantified. The tendon–bone histological evaluation results varied with the selection of the femur or tibia side tunnel, which the healing in the tibial tunnel was inferior to that in the femoral tunnel [25] and were also affected by the selected tunnel site, which the graft-tunnel motion was greatest at the tunnel apertures and least at the tunnel exit [26]. Therefore, in this research, only the sections containing the middle portion of bone tunnels from femur side samples were used for evaluation.

Fluorescence Evaluation

The intra-articular graft samples implanted with eGFP-labeled BMSCs underwent fluorescence examination. First, the samples were fixed in 4% paraformaldehyde (diluted in PBS) for 20 minutes and washed with PBS twice for 5 minutes. Thereafter, the samples were dehydrated with 10% sucrose for 1 hour, embedded in optimum cutting temperature compound, and frozen completely in a −20°C freezer. The 5-μm-thick frozen sections were cut with Leica CM1900 Cryostat (Leica, Heidelberger, Germany), counterstained with 4′, 6-diamidino-2-phenylindole for 5 minutes in a black box, and sealed with neutral balsam. Prompt fluorescence examination was performed using ×200 magnification via fluorescence microscopy (Leica DMI4000B, Wetzlar, Germany). The positive cells and area of all images of each animal were summed up and normalized to ×200 field.

Immunohistochemical Evaluation

The eGFP-labeled BMSCs in the tendon–bone paraffin section were detected by immunohistochemical staining according to a published protocol [27]. The main reagents in the process included specific rabbit polyclonal anti-GFP antibody (Abcam, Cambridge, MA; dilution, 1:500), goat anti-rabbit polyclonal immunoglobulin G horseradish peroxidase-conjugated secondary antibody (Abcam; dilution, 1:100), and DAB Substrate Kit (Abcam, Cambridge, MA). The sections were counterstained with hematoxylin. Six to eight images were obtained via light microcopy (DM2500; Leica, Solms, Germany) using ×200 magnification for each sample. The positive cells and area of all images of each animal were summed up and normalized to ×200 field. One trained independent investigator blinded to the trial design analyzed all the images in a descriptive manner.

Micro-CT Evaluation

According to a previously published micro-CT scanning and evaluating protocol by Wen et al. [28], all the femoral condyle samples were scanned with a resolution of 18 μm using a SkyScan 1,176 Scanning System (Nanovea, Pasadena, CA) at 80 kV/300 μA. The scanning region covered the whole length of the bone tunnels. After obtaining two-dimensional image slices, a cylindroid region of interest (ROI) with 4.0 mm diameter (in the sagittal view) and 5.0 mm length (in the coronal view) was user-defined to cover bone tunnel and was used for subsequent analysis (Fig. 1C, 1D). Slices without bone surrounding all sides of the bone tunnel defect were excluded. The ROI was uniformly delineated, and three-dimensional reconstructions were performed using gauss = 0.8, sigma = 1, and threshold = 210 throughout the analyses. The bone histomorphometric parameters for the femoral bone tunnel, including bone mineral density (BMD), measured in milligrams of hydroxyapatite (HA) per cubic centimeter [mg HA/cm^3]), and bone volume/total volume (BV/TV) with a CT Analyzer Version 1.13.2.1 (CTAn, Bruker Micro-CT, Kontich, Belgium).

Mechanical Evaluation

Mechanical analysis of the femur-ACL graft-tibia was performed in accordance with an established pattern [29] using an Instron distraction machine (3,345, Instron Corp., Canton, MA). The samples stored in −80°C were completely thawed at room temperature. The soft tissues around the knee joint were carefully dissected, leaving approximately 5-cm-long bone shafts at each side and intact ACL graft. The samples were mounted onto the machine with the knees at 30–45° flexion, ensuring that the bone tunnels were oriented along the direction of the tensile load. The suspending sutures used to fix the graft were disconnected before testing. The femur-graft-tibia complex was loaded at a velocity of 5 mm/min until graft failure. The load deformation curve was recorded, from which the ultimate load to failure and stiffness were measured. The failure mode characterized as graft pull-out from the bone tunnel or graft rupture in the joint cavity was recorded. The stiffness of the graft was measured by Microstrain DVRT machine (#M-DVRT-3-BX-SK2, Minneapolis, MN) automatically. The data were gathered from linear load deformation curve.

Statistical Analysis

The BMD, BV/TV, ultimate load, and stiffness data were expressed as the mean ± standard deviation. Student's *t* test was used for data comparison between the experimental and control groups at each time point with SPSS analysis software (version 17.0; SPSS Inc., an IBM Company, Chicago, IL). Statistical significance was set at $p < .05$.

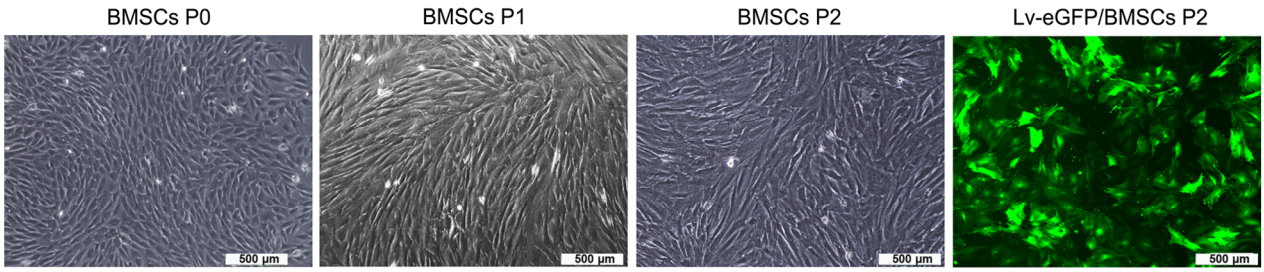

Figure 2. Representative images of BMSCs at various passages and the eGFP tagged BMSCs before implantation (×200). Abbreviations: BMSCs, bone marrow-derived mesenchymal stem cells; Lv-eGFP, lentivirus vector expressing enhanced green fluorescent protein.

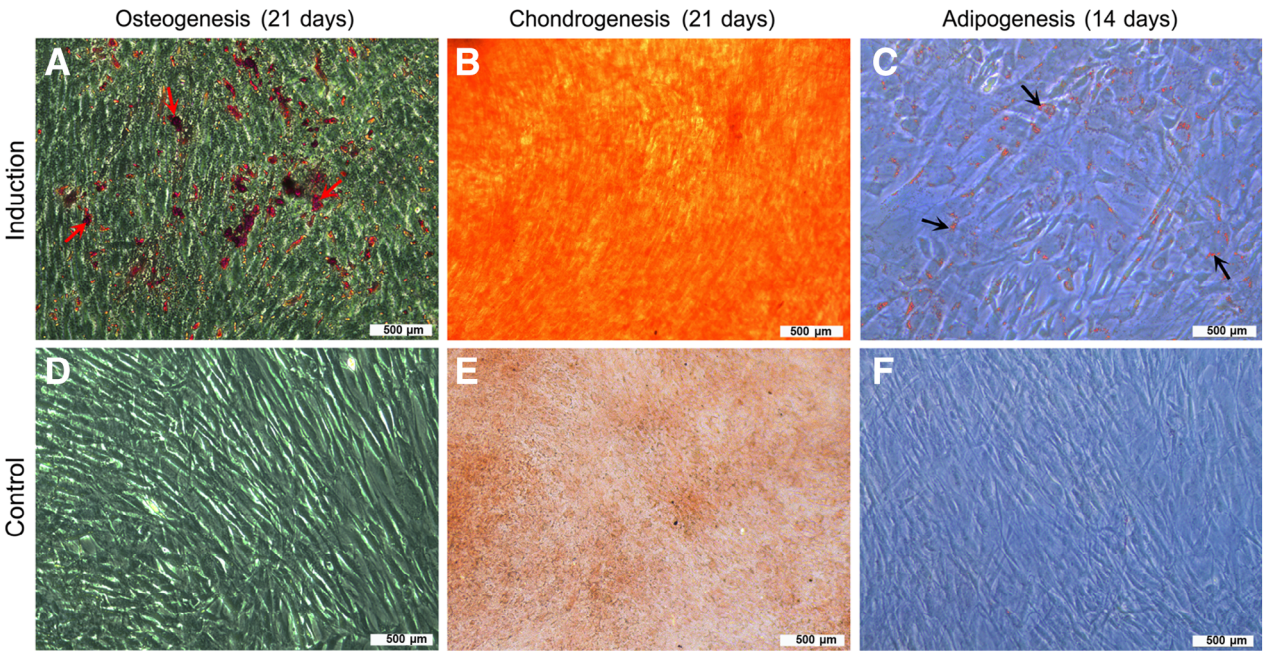

Figure 3. Representative images of three lineage differentiation of bone marrow-derived mesenchymal stem cells. **(A, C, D, F)**: ×200; **(B, E)** ×100. Red arrowheads marked calcium nodules. Black arrowheads marked lipid droplets in cellular plasma.

RESULTS

Histology

BMSC Morphology and lv-eGFP Transfection In Vitro

The BMSCs from the original passage to passage 2 maintained the typical spindle shape of a single BMSC and the whirlpool arrangement type of BMSC colony. Using Lv-eGFP transfection, the main BMSCs obtained eGFP labels. The eGFP-positive cells were used for implanted BMSC tracing analysis (Fig. 2).

Three Lineage Differentiation of BMSCs In Vitro

The BMSCs in passage 3 showed remarkable effects in osteogenesis, chondrogenesis, and adipogenesis after corresponding induction for some days. A significant difference was observed when comparing these BMSCs with the control samples cultured in normal growth culture medium (Fig. 3).

Tracing Examination of eGFP-Labeled BMSCs

The eGFP-positive cells were observed at all three time points in both intra-articular and intraosseous portions (Fig. 4A–4F). The number of detectable eGFP-positive cells decreased over time: 30.03 ± 4.92 (week 4) versus 16.36 ± 2.35 (week 8) versus 3.32 ± 0.74 (week 12) at the intra-articular samples; 23.21 ± 4.35 (week 4) versus 15.12 ± 3.45 (week 8) versus 12.28 ± 2.83 (week 12) at the intraosseous samples (Fig. 4G, 4H). Especially at the intra-articular samples, via fluorescence detection, which the pairwise comparison was significantly different between each two time points ($p < .05$). And the eGFP-positive cell number in week 4 was significantly higher than that in week 8 and week 12 ($p < .05$).

H&E and Polarized Microscopy Evaluation of the Intra-Articular Portion

After sacrifice, the allograft was exposed for observation of integrity and stability. We did not detect any secondary allograft rupture or loosening in each case. The tendon–bone complex samples were collected for further evaluations.

At week 2, the BMSC/DA groups (Fig. 5E) exhibited considerable fibroblast growth into a number of layers of graft midsubstance. The outer layers presented higher cellular density than the inner layers. The FFA groups showed only a few scattered fibroblast growth into the superficial layers (Fig. 5A). No vascular-like structures were found in both groups. High content of collagen birefringence was maintained in most areas in

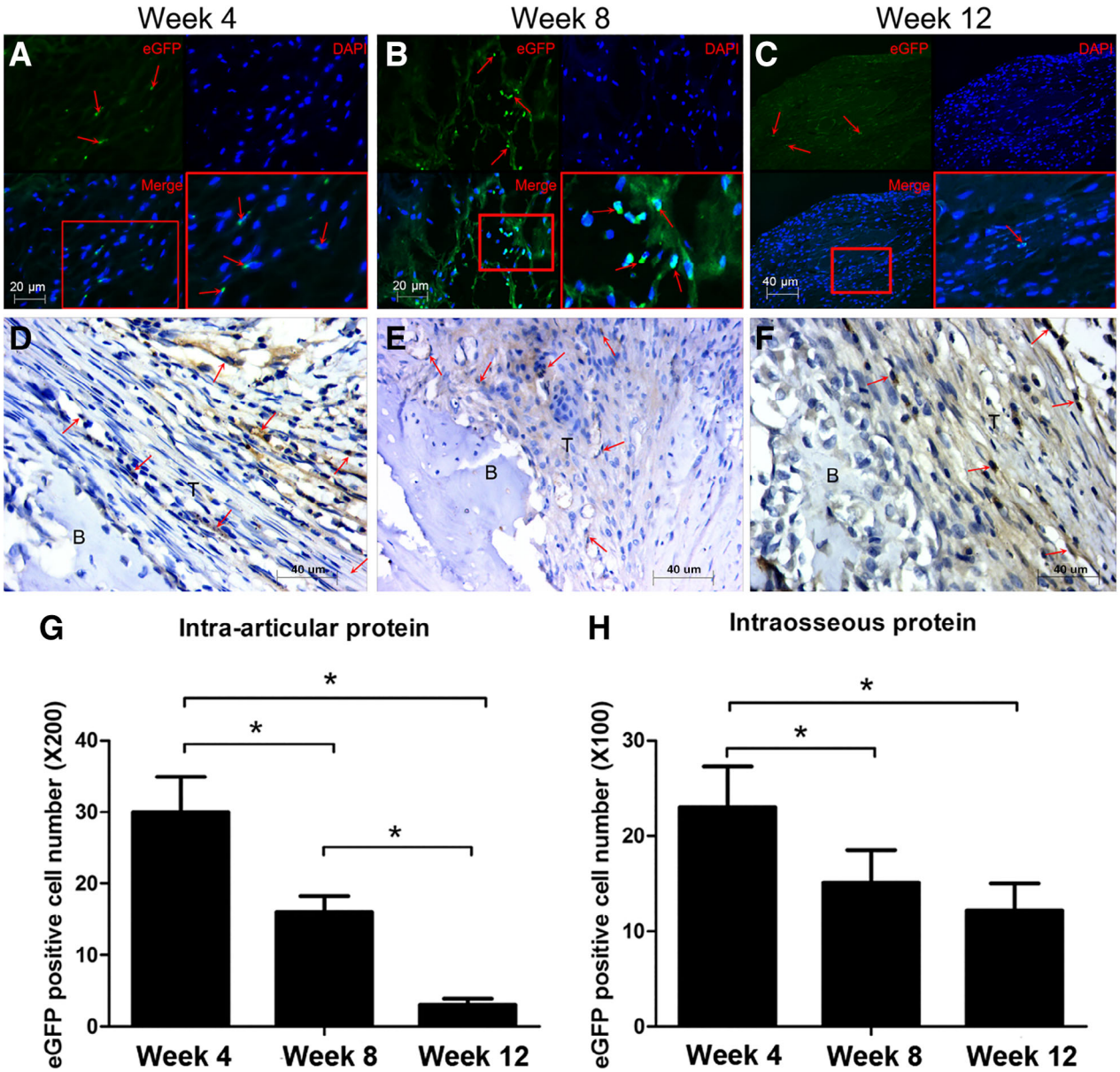

Figure 4. Representative images and quantification of eGFP-positive cells in both intra-articular portion and intraosseous portion (N = 2/time point). **(A, B, D, E, F):** ×200; **(C)** ×100. **(A–C):** Fluorescence images of intra-articular portion sections. **(D–F):** Immunohistochemistry images of tendon–bone portion sections. Insets show enlarged view of expressed eGFP. The red arrowheads marked the eGFP-positive cells. **(G):** In intra-articular portion, the eGFP-positive cell number in week 4 was significantly higher than that in week 8 and week 12, and the eGFP-positive cell number in week 8 was significantly higher than that in week 12 ($p < .05$). **(H):** In intraosseous portion, the eGFP-positive cell number in week 4 was significantly higher than that in week 8 and week 12 ($p < .05$). Abbreviations: B, bone portion; DAPI, 4′,6-diamidino-2-phenylindole; eGFP, enhanced green fluorescent protein; T, tendon portion.

both groups. In BMSC/DA samples, areas with cell infiltration showed low content of collagen birefringence, whereas the acellular areas showed higher signals (Fig. 5E) than the areas with cell infiltration.

At week 4, in the BMSC/DA group, the cellular quantity increased and almost achieved complete ingrowths into the graft midsubstance (Fig. 5F). Collagen birefringence was distributed broadly; however, some were distributed disorderedly. In the FFA group, cellular ingrowths increased as well, and large areas of acellular zones (Fig. 5B) remained. Collagen birefringence in the FFA group showed similar features to that in the BMS/DA group at week 2, that is, hypercellular areas demonstrated low content of birefringence and acellular areas showed high signals (Fig. 5B). Newly formed vascular structures began occurring in both groups but had higher frequency in the BMSC/DA group than in the FFA group (Fig. 5F, black arrowheads).

At week 8, the BMSC/DA and FFA groups accomplished almost full cellular ingrowths with multiple blood vessel formation. Cellularity in the FFA group was more mature than that in the BMSC/DA group. The BMSC/DA group contained more linearly shape nuclei than the FFA group (Fig. 5G), whereas the FFA group had more spindle-shaped nuclei than the BMSC/DA group (Fig. 5C). Collagen birefringence content was higher and more regular in the BMSC/DA group than in the FFA group (Fig. 5G).

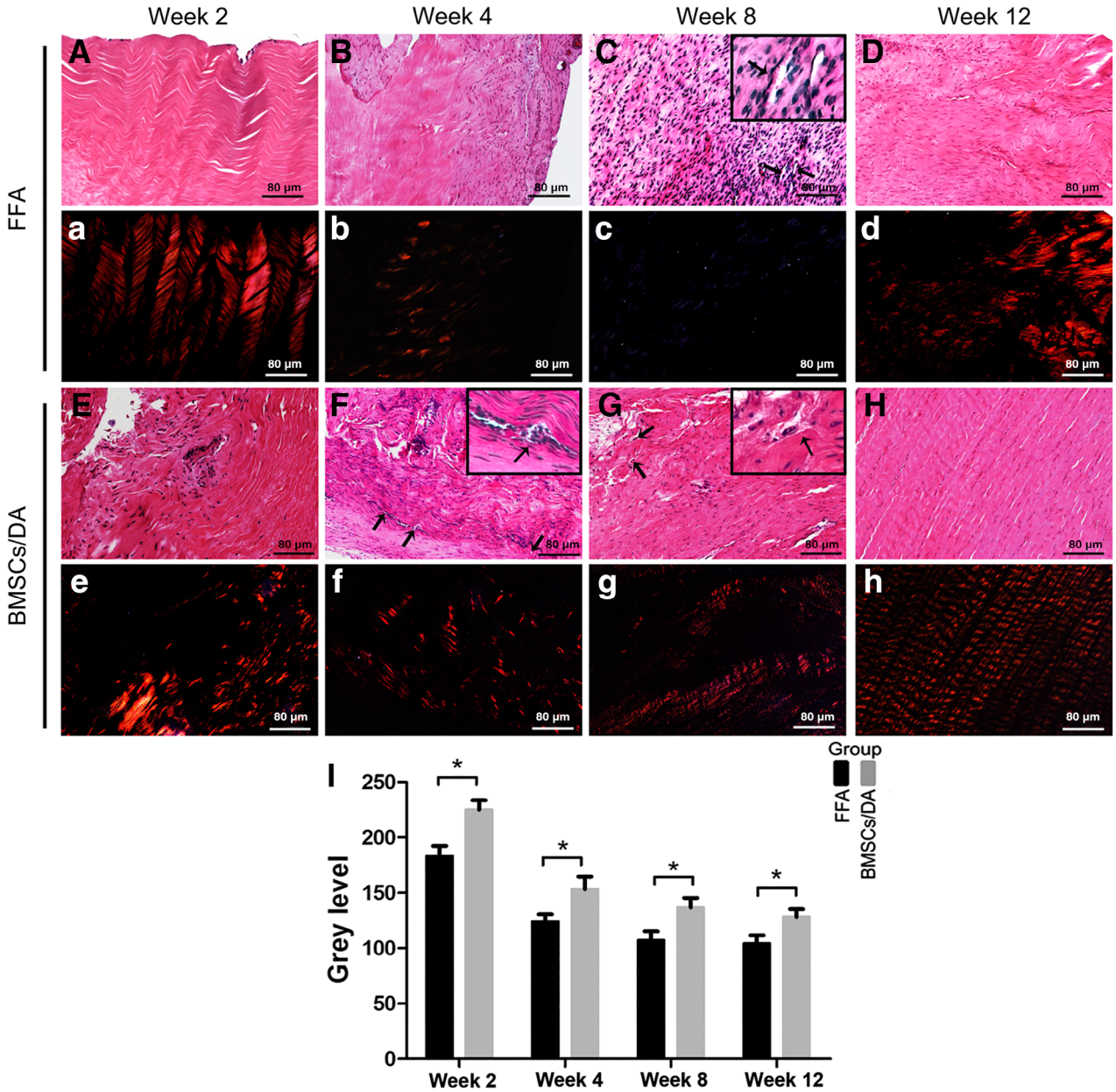

Figure 5. Representative histological images and quantification of level of collagen birefringence expression in intra-articular portion of FFA group and BMSCs/DA group (N = 5/group/time point). **(A–H):** H&E staining. **(a–h):** Corresponding polarized images (×100). **(I):** Quantification of level of collagen birefringence expression in FFA group and BMSCs/DA group. Black arrowheads marked blood vessels. *, $p < .05$. Scale bar = 80 μm for all images. Abbreviations: BMSCs, bone marrow-derived mesenchymal stem cells; DA, decellularized allograft; FFA, fresh frozen allograft.

However, it was ultimately lower in the FFA group even with full cellular ingrowth (Fig. 5C).

At week 12, no significant difference was observed at the cellular state and blood vessel composition. Most of the cells were arranged in lines with the collagen matrix, and a low quantity of blood vessels was scattered in the midsubstance (Fig. 5D, 5H). However, polarized microscopy showed that collagen birefringence in the BMSC/DA group was arranged more regularly and broadly than that in the FFA group (Fig. 5D, 5H).

The quantification of level of collagen birefringence expression showed higher content of collagen birefringence in BMSC/DA groups than the FFA group at all time points (Fig. 5I; $p < .05$): 225.17 ± 8.49 versus 182.24 ± 9.13 (week 2); 153.27 ± 11.32 versus 124.05 ± 6.63 (week 4); 136.73 ± 8.84 versus 107.11 ± 8.21 (week 8); and 125.49 ± 6.87 versus 104.32 ± 7.36 (week 12).

M-T Staining for Intraosseous Portion

At week 2, the FFA group presented scarce newly formed fibrovascular tissues at the tendon–bone interface, and the graft in the bone tunnel was almost acellular. The BMSC/DA group demonstrated abundant-activated proliferation of fibrovascular tissues at the tendon–bone interface. Moreover, newly formed fibroblasts and blood vessels infiltrated into the graft midsubstance (Fig. 6A, 6E).

At week 4, the FFA group gained more newly proliferated fibrovascular tissues at the tendon–bone interface than those

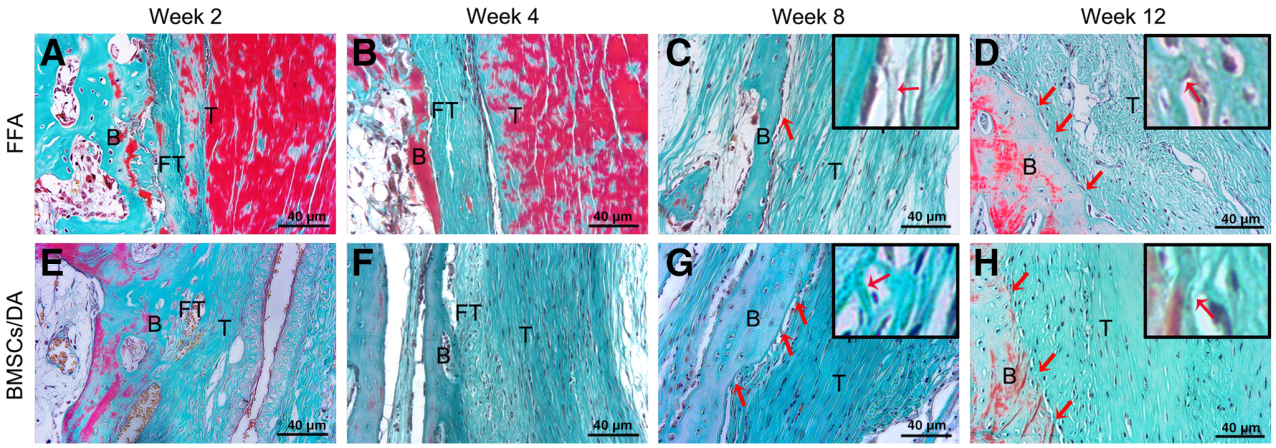

Figure 6. Representative histological images of intraosseous portion of FFA group and BMSCs/DA group (Masson trichrome staining, ×200; *N* = 5/group/time point). Intraosseous portion at Week 2 **(A)**, Week 4 **(B)**, Week 8 **(C)**, and Week 12 **(D)** in FFA group. Intraosseous portion at Week 2 **(E)**, Week 4 **(F)**, Week 8 **(G)**, and Week 12 **(H)** in BMSCs/DA group. Red arrowheads marked the Sharpey fibers. *, $p < .05$. Scale bar = 40 μm for all images. Abbreviations: B, bone; BMSCs, bone marrow-derived mesenchymal stem cells; DA, decellularized allograft; FFA, fresh frozen allograft; FT, fibrovascular tissues; T, tendon graft.

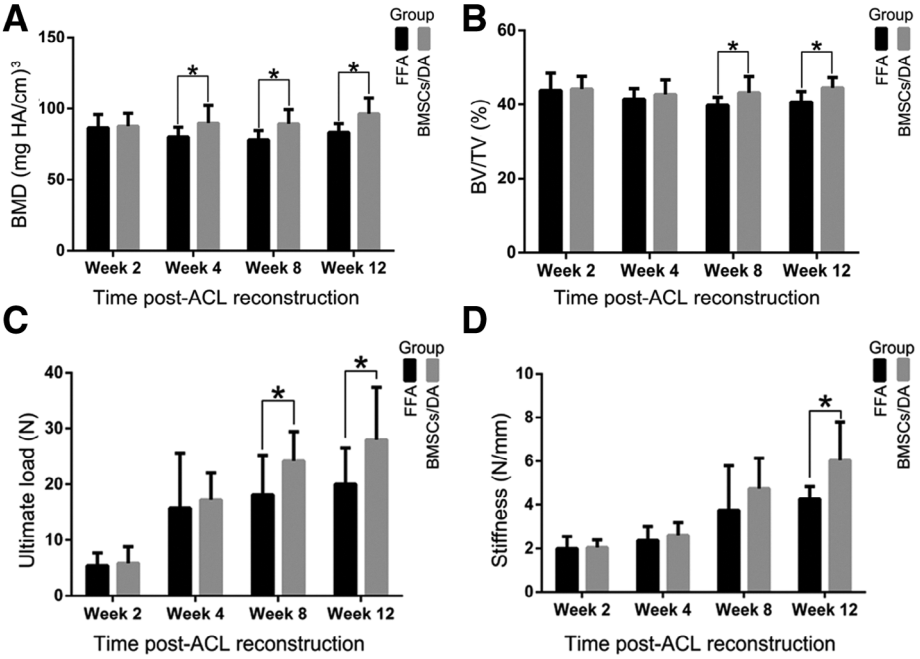

Figure 7. The microcomputed tomography evaluation and mechanical testing analysis of FFA group and BMSCs/DA group (*N* = 5/group/time point). **(A):** BMD (mg HA/cm^3) of the femoral region of interest (ROI). **(B):** BV/TV of the femoral ROI. **(C):** Ultimate load (N). **(D):** Stiffness (N/mm). *, $p < .05$. Abbreviations: ACL, anterior cruciate ligament; BMD, bone mineral density; BMSCs, bone marrow-derived mesenchymal stem cells; BV/TV, bone volume/total volume; DA, decellularized allograft; FFA, fresh frozen allograft.

formed at week 2. However, these tissues were still arranged in a loose, disordered manner. Few graft fiber superficial layers exhibited fibroblast ingrowth, and most of the graft remained acellular. The BMSC/DA group achieved sufficient fibroblast infiltration into the graft. Fibrovascular tissues became denser than those at week 2, thereby binding the graft tightly to the bone tunnel (Fig. 6B, 6F).

At week 8, the quantity of fibroblasts in the FFA graft increased compared with that at week 4. Fibrovascular-like tissues at the tendon–bone interface disappeared, and some newly formed Sharpey's fibers occurred, which were still thin and scarce (Fig. 6C, marked as red arrowheads). In the BMSC/DA group, newly formed Sharpey's fibers in the tendon–bone interface appeared thicker and stronger than those in the FFA group (Fig. 6G, marked as red arrowheads). However, these fibers were still arranged in a loose manner.

At week 12, intraosseous grafts were anchored onto the bone walls with classical, densely compacted Sharpey's fibers in both groups (Fig. 6D, 6H). No significant difference could be easily justified by histological evaluation.

Micro-CT Analysis

For BMD (mg HA/cm^3), the data were presented in the format of the FFA group versus the BMSC/DA group as follows: week

Table 1. Failure mode of femur-graft-tibia complex during mechanical testing

Time points	Groups (*n*)	Tunnel pullout		Intra-articular midsubstance failure
		Femur side	Tibia side	
Week 2	FFA (10)	4	6	0
	BMSCs/DA (10)	7	3	0
Week 4	FFA (10)	0	3	7
	BMSCs/DA (10)	0	0	10
Week 8	FFA (10)	0	0	10
	BMSCs/DA (10)	0	0	10
Week 12	FFA (10)	0	0	10
	BMSCs/DA (10)	0	0	10

Abbreviations: BMSCs/DA, decellularized allograft combined with bone marrow-derived mesenchymal stem cells; FFA, fresh frozen allograft.

2, 86.46 ± 9.50 versus 87.52 ± 9.32 (F = 0.01, p = .80); week 4, 80.20 ± 6.55 versus 89.70 ± 12.43 (F = 2.40, p = .04); week 8, 78.15 ± 6.42 versus 89.24 ± 10.08 (F = 1.76, p < .01); and week 12, 83.26 ± 6.05 versus 96.43 ± 11.11 (F = 5.90, p < .01; Fig. 7A). The BMSC/DA group had significantly higher BMD than the FFA group at weeks 4, 8, and 12.

For BV/TV (%), the data of the FFA group versus the BMSC/DA group at the four time points from week 2 to week 12 were 43.76 ± 4.78 versus 44.18 ± 3.52 (F = 3.25, p = .83), 41.48 ± 2.78 versus 42.72 ± 3.99 (F = 2.46, p = .43), 39.80 ± 2.19 versus 43.18 ± 4.46 (F = 6.81, p = .04), and 40.68 ± 2.79 versus 44.47 ± 2.89 (F = 0.02, p < .01; Fig. 7B). The BMSC/DA group achieved significantly higher BV/TV than the FFA group at weeks 8 and 12.

Mechanical Testing Analysis

The failure mode characterized as graft pull-out from the bone tunnel or graft rupture in the joint cavity was recorded in Table 1. The ultimate load data for the FFA group versus the BMSC/DA group at the four time points were as follows: week 2, 5.39 ± 2.31 versus 5.82 ± 2.98 (F = 1.04, p = .72); week 4, 15.72 ± 9.88 versus 17.18 ± 4.91 (F = 1.64, p = .68); week 8, 18.16 ± 7.02 versus 24.19 ± 5.22 (F = 0.42, p = .04); and week 12, 20.01 ± 6.52 versus 27.97 ± 9.42 (F = 3.54, p = .04; Fig. 7C). The BMSC/DA group had significantly higher ultimate load than the FFA group at weeks 8 and 12.

For stiffness (N/mm), the data of the FFA group versus the BMSC/DA group were recorded as follows: week 2, 2.00 ± 0.55 versus 2.05 ± 0.34 (F = 2.80, p = .82); week 4, 2.36 ± 0.64 versus 2.60 ± 0.57 (F = 0.06, p = .39); week 8, 3.75 ± 2.05 versus 4.74 ± 1.39 (F = 2.42, p = .22); and week 12, 4.26 ± 0.57 versus 6.04 ± 1.74 (F = 11.79, p < .01; Fig. 7D). The BMSC/DA group achieved significantly higher stiffness than the FFA group only at week 12.

Discussion

As a cell source with multiple differentiation potential, BMSCs have been widely studied in musculoskeletal diseases repair [14–18]. The detailed cell application protocols included injection [30, 31], coculture in vitro [32], with collagen gel or fibrin glue carrier [16, 19], combination with some tissue-engineered scaffold [33], and cell sheet technology [34, 35]. However, no widely accepted standard on seed cell application in tissue engineering experiments is available. In this research, the combination of a decellularized ST scaffold with autologous BMSCs was applied in ACL reconstruction surgery with a rabbit model. The autologous BMSCs were delivered to the recipient site in two ways. On the one hand, 1 ml of BMSC suspension in PBS was simultaneously injected into the midsubstance and seeded on the surface of one decellularized graft. Through this method, the BMSCs were imbedded into the apertures of the decellularized graft (Fig. 1B). We found that 1 ml of suspension was sufficient to achieve full hydration for one piece of freeze-dried decellularized ST graft. On the other hand, the remaining 1 ml of suspension was injected into the bone tunnels with a syringe. Inevitably, some suspension leaked into the joint cavity. Subsequently, prompt ACL reconstruction with BMSC-seeded decellularized ST scaffold was performed. This complex BMSC delivery method presented several advantages. First, it ensured that activated BMSCs were offered at the moment of surgery and reduced the chance uncontrolled differentiation because of the detailed collagen scaffold microenvironment and high cellular density conditions during in vitro culture. Second, using this method, the BMSCs were simultaneously delivered to both the tendon–bone interface and graft midsubstance. The seed cells were reserved in double states, that is, one as free cells distributed into the bone tunnels and joint cavity and another as relatively fixed seed cells embedded in the graft because the varied microenvironments played appropriate roles for BMSCs differentiating into the best suitable cell lines. Third, the BMSC application method applied in this research is simple and easy to operate in future clinical surgery. Finally, it may reduce the potential incidence of contamination by pathogenic microorganisms from the external environment because of the long coculture time in vitro. Moreover, the initial high quantity of seed cells was guaranteed. eGFP-labeled BMSC tracing examination revealed eGFP-positive cells in both bone tunnels and intra-articular graft from week 4 to week 12 after the surgery. This result confirmed the feasibility and effectivity of the cell application method used in this study.

The intra-articular part of the BMSC/DA graft achieved superior histology results than the FFA graft in terms of rapid fibroblast infiltration and blood vessel formation. Guo et al. have shown that BMSCs transplantation significantly enhanced angiogenesis in brain tissues after traumatic brain injury via upregulation of vascular endothelial growth factor and angiogenin-1 [36]. Moreover, Notch signaling was found to be activated with transplantation of preconditioned BMSCs in rat lungs suffering from injury [37]. These might partially explain the improved histology we observed in BMSC/DA graft. Superiority at the cellular populations was attributed to two possible reasons. One was the original autologous BMSCs seeded in the decellularized graft. Using this method, activated BMSCs were initially located in the graft, and no activated cells were observed in the fresh frozen allograft. The survival of implanted BMSCs was proven by eGFP tracing examination from week 4 to week 12 after the surgery. This result was similar to the findings of Lui et al. [34]. In their research, the autograft wrapped with GFP-tagged BMSC sheet was used for ACL reconstruction, and GFP-positive cells were observed at weeks 2, 6, and 12 after surgery. Similar results on implanted BMSC tracing examination were also achieved by Li et al. with an extra articular tendon–bone healing rat model [30].

With regard to the tendon–bone healing evaluation, a significant difference between the femur and tibia side bone tunnels

was widely believed. Moreover, various sites in the same bone tunnel considerably differed. Tendon-bone healing at the femoral bone tunnel was believed to be superior to the tibia bone tunnel [25]. At the same bone tunnel, tendon–bone healing at the tunnel exit was better than that at the tunnel entrance [26]. Thus, to avoid the variance caused by the selected site, we only evaluated the middle site of the femoral bone tunnel in this study. Thus, the interference from the inherent fibrocartilage tissues near the tunnel entrance was neglected. In this study, tendon-bone healing evaluation obeying this criterion revealed no newly formed fibrocartilage tissues both in the FFA and BMSC/DA groups. Autologous grafts could achieve relatively easier fibrocartilage formation at the tendon-bone interface than allograft. Nonetheless, no fibrocartilage tissues were observed with a rabbit extraarticular tendon–bone healing model at week 6 after the surgery in Liu et al.'s research [38]. In Panni et al.'s research on a rabbit ACL model with autologous patellar tendon graft, a thin layer of fibrocartilage tissues was witnessed at the tendon-bone interface at 12 weeks after surgery [39]. Fibrocartilage formation was hard to detect in the allogenic tendon graft at the corresponding period. For example, Soon et al. obtained similar results to our findings on the allograft group, indicating that only Sharpey's fiber formation was observed 8 weeks after the surgery in a rabbit ACL reconstruction model with Achilles tendon allografts [19]. The same tendon–bone healing result was also obtained in a 2.5-year human case with allogenic freeze-dried tendon graft [40]. However, a distinguishable result was obtained by Soon et al.; in their study, when the allograft was wrapped with autogenous BMSCs in a fibrin glue carrier, BMSC-enhanced reconstructions exhibited a large collection of cartilage cells lining at the tendon–bone interface at 2 weeks, a chondroosteoid-like structure at 4 weeks, and a mature zone of fibrocartilage blending from bone to allograft at 8 weeks [19]. No BMSC trace examination was performed in their study. Thus, the relationship between the newly formed fibrocartilage and seeded BMSCs was difficult to determine.

Collagen birefringence measured with polarized microscopy was usually used to evaluate the collagen matrix remodeling process [34, 41, 42]. The mature collagen matrix presented high amount of and regular birefringence, whereas newly formed collagen matrix demonstrated fewer amount of birefringence with irregular shape. As shown in the allograft group, the primarily implanted graft had high content of collagen birefringence even without fibroblast ingrowth at week 2. With cell infiltration into the midsubstance, the original collagen matrix was metabolized, and the corresponding collagen birefringence symbol showed no or less birefringence in the hypercellular zone and with relatively more birefringence in the acellular zone. This phenomenon was observed at week 4 in the allograft group. Along with more cell ingrowths, the allograft became almost completely cellularized at week 8, and the original collagen matrix experienced vigorous metabolism. Newly formed collagen matrix was still disordered. Thus, collagen birefringence was at ultimate low levels. With further remodeling of the extra cellular matrix, the allograft's collagen birefringence was partially recovered at week 12. However, in the BMSC/DA group, the collagen matrix remodeling process was accelerated with the early fibroblast ingrowths and blood vessel formation. Moreover, higher content of collagen birefringence was achieved at week 12 after the surgery. This phenomenon was also observed by Lui et al. [34]. In their research, the BMSC sheet-wrapped autograft showed quick collagen birefringence recovery than the autograft group. This result may be due to low antigenicity, porous structure of the scaffold, and original implanted BMSCs in the BMSC/DA group. On the one hand, superior physicochemical features of the decellularized allograft induced early host cell infiltration. On the other hand, the seeded autologous BMSCs neglected this process theoretically. Ultimately, these cells accelerated the collagen matrix remodeling process. Considering the factors such as high antigenicity and dense collagen barricade in the allograft group, the collagen remodeling process was overwhelmingly hindered.

For BMD and BV/TV, a gradual decrease in the allograft group was observed 2 weeks after the surgery; this trend was reversed only until the 12th week. However, the BMSC/DA group showed a relatively different developing trend; a consistent increase was maintained to the final observation time point. A similar result was reported by Wen et al. in a rabbit ACL reconstruction model with autograft [28], indicating that preliminary BMD loss and microarchitecture deterioration should be attributed to the activated osteoclasts accumulated at the tunnel surface at the earlier period after the surgery. This opinion was also supported by other studies [28, 43, 44]. For the allogenic graft, immune rejection was thought to be another important factor for poor new bone formation in the bone tunnel [45]. Immune cells such as T lymphocytes, B cells, and natural killer cells were detected in various tissue allografts [46–48]. For tissue-engineered grafts in the BMSC/DA group, most antigen components were depleted via decellularization. Thus, low immune rejection response was expected. The BMSCs were believed to have immunomodulatory function, and they could suppress mixed lymphocyte reaction and attenuate alloresponses [49]. BMSCs were known to secrete a variety of cytokines that can suppress the proliferation of immune cells including B cells and T cells. BMSCs also inhibit the maturation of monocytesand promote the skewed phenotypic differentiation of M2 macrophages [50]. Theoretically, as a stem cell, implanted BMSCs can differentiate into osteoblasts, thereby promoting new bone formation.

Mechanical transformation was correlated with graft remodeling and tendon–bone healing. No sufficiently strong tendon-bone connection was observed at week 2 after the surgery in the two groups. Thus, the failure mode was at the bone tunnel with minimum data. In addition to the tendon–bone healing reinforcement and the degradation of graft in the joint cavity, the failure mode was transferred to the graft midsubstance. With strong Sharpey's fiber formation in the bone tunnel, mechanical strength was promoted. Similar transformation of the failure mode was also observed by other studies [20, 35, 51].

This study had some limitations. First, the sample size was not yet large enough to counteract the variation in data. Thus, the chance of making a second-type error was unavoidable. Although both sides of knee joint were used in the BMSC tracing, the sample number was relatively small. Second, seed cells were implanted in a complex manner. They were not only seeded in decellularized scaffold but also directly injected into the bone tunnels. Thus, deciding which part of the implanted cells served as the main force was difficult. Third, the seed cell quantity applied in this research was determined in accordance with the previous data, and the optimum dose was still unknown in this appropriate protocol. Fourth, this study was a short-duration analysis (within 12 weeks), so the difference between the two groups in a long duration and whether the BMSC/DA graft can achieve ultimate fibrocartilage connection

remain unknown. Fifth, bilateral ACL reconstruction was performed in this study, which might cause increased lameness of the animals due to the surgery induced affection to the joint movement. Lastly, the property of birefringence of normal ACL, the mechanisms for BMSC/DA graft inducing early fibroblast infiltration and blood vessel formation were not involved; the roles individually played by BMSCs and decellularized scaffold still need further exploration. Further research should be carried out to study these unsolved problems.

Conclusion

The decellularized allogenic tendon graft combined with autologous BMSCs used in this study achieved superior ligamentization, stronger tendon–bone healing, and better bone tunnel wall ossification after ACL reconstruction in the rabbit model than fresh frozen free tendon allograft.

Acknowledgments

This study was funded by National Natural Science Foundation of China (81301547), Guangdong Provincial Science and Technology Grant (2015A030401017), and Health and Family Planning Commission of Shenzhen Municipality (SZBC2017022).

Author Contributions

W.L.: performed the experiments, conception/design, prepared the manuscript, tables, and figures, final approval of manuscript; S.D.: performed the experiments, prepared the manuscript, tables, and figures, final approval of manuscript; G.X., X.H., X.L., Z.Y., H.L.: performed the experiments, final approval of manuscript; Z.D.: conception/design, revised the manuscript, final approval of manuscript; J.Z.: conception/design, final approval of manuscript; J.X.: prepared the manuscript, tables, and figures, revised the manuscript, final approval of manuscript; P.S.: prepared the manuscript, tables, and figures, final approval of manuscript; S.Y.: revised the manuscript, final approval of manuscript; Y.Z.: final approval of manuscript.

Disclosure of Potential Conflicts of Interest

The authors indicated no potential conflicts of interest.

References

1 Cohen SB, Sekiya JK. Allograft safety in anterior cruciate ligament reconstruction. Clin Sports Med 2007;26:597–605.

2 Dheerendra SK, Khan WS, Singhal R et al. Anterior cruciate ligament graft choices: A review of current concepts. Open Orthop J 2012;6:281–286.

3 Vorlat P, Verdonk R, Arnauw G. Long-term results of tendon allografts for anterior cruciate ligament replacement in revision surgery and in cases of combined complex injuries. Knee Surg Sports Traumatol Arthrosc 1999;7:318–322.

4 Noyes FR, Barber-Westin SD. Reconstruction of the anterior cruciate ligament with human allograft. Comparison of early and later results. J Bone Joint Surg Am 1996;78:524–537.

5 Gulotta LV, Rodeo SA. Biology of autograft and allograft healing in anterior cruciate ligament reconstruction. Clin Sports Med 2007; 26:509–524.

6 Prodromos C, Joyce B, Shi K. A meta-analysis of stability of autografts compared to allografts after anterior cruciate ligament reconstruction. Knee Surg Sports Traumatol Arthrosc 2007;15:851–856.

7 Scheffler SU, Schmidt T, Gangey I et al. Fresh-frozen free-tendon allografts versus autografts in anterior cruciate ligament reconstruction: Delayed remodeling and inferior mechanical function during long-term healing in sheep. Art Ther 2008;24:448–458.

8 Snyder SJ, Arnoczky SP, Bond JL et al. Histologic evaluation of a biopsy specimen obtained 3 months after rotator cuff augmentation with Graft Jacket Matrix. Art Ther 2009;25:329–333.

9 Eastlund T. Bacterial infection transmitted by human tissue allograft transplantation. Cell Tissue Bank 2006;7:147–166.

10 Tugwell BD, Patel PR, Williams IT et al. Transmission of hepatitis C virus to several organ and tissue recipients from an antibody-negative donor. Ann Intern Med 2005;143:648–654.

11 Gilbert TW. Strategies for tissue and organ decellularization. J Cell Biochem 2012; 113:2217–2222.

12 Gilbert TW, Sellaro TL, Badylak SF. Decellularization of tissues and organs. Biomaterials 2006;27:3675–3683.

13 Whitlock PW, Seyler TM, Parks GD et al. A novel process for optimizing musculoskeletal allograft tissue to improve safety, ultrastructural properties, and cell infiltration. J Bone Joint Surg Am 2012;94:1458–1467.

14 Bruder SP, Jaiswal N, Ricalton NS et al. Mesenchymal stem cells in osteobiology and applied bone regeneration. Clin Orthop Relat Res 1998;Suppl;355S:S247–S256.

15 Gupta PK, Das AK, Chullikana A et al. Mesenchymal stem cells for cartilage repair in osteoarthritis. Stem Cell Res Ther 2012;3:25.

16 Ouyang HW, Goh JC, Thambyah A et al. Knitted poly-lactide-co-glycolide scaffold loaded with bone marrow stromal cells in repair and regeneration of rabbit Achilles tendon. Tissue Eng 2003;9:431–439.

17 Ge Z, Goh JC, Lee EH. The effects of bone marrow-derived mesenchymal stem cells and fascia wrap application to anterior cruciate ligament tissue engineering. Cell Transplant 2005;14:763–773.

18 Ouyang HW, Goh JC, Lee EH. Use of bone marrow stromal cells for tendon graft-to-bone healing: Histological and immunohistochemical studies in a rabbit model. Am J Sports Med 2004;32:321–327.

19 Soon MY, Hassan A, Hui JH et al. An analysis of soft tissue allograft anterior cruciate ligament reconstruction in a rabbit model: A short-term study of the use of mesenchymal stem cells to enhance tendon osteointegration. Am J Sports Med 2007;35:962–971.

20 Grana WA, Egle DM, Mahnken R et al. An analysis of autograft fixation after anterior cruciate ligament reconstruction in a rabbit model. Am J Sports Med 1994;22:344–351.

21 Tang JB, Cao Y, Zhu B et al. Adeno-associated virus-2-mediated bFGF gene transfer to digital flexor tendons significantly increases healing strength. An in vivo study. J Bone Joint Surg Am 2008;90:1078–1089.

22 Tischer T, Vogt S, Aryee S et al. Tissue engineering of the anterior cruciate ligament: A new method using acellularized tendon allografts and autologous fibroblasts. Arch Orthop Trauma Surg 2007;127:735–741.

23 Tischer T, Aryee S, Wexel G et al. Tissue engineering of the anterior cruciate ligament-sodium dodecyl sulfate-acellularized and revitalized tendons are inferior to native tendons. Tissue Eng Part A 2010;16:1031–1040.

24 Kohno T, Ishibashi Y, Tsuda E et al. Immunohistochemical demonstration of growth factors at the tendon-bone interface in anterior cruciate ligament reconstruction using a rabbit model. J Orthop Sci 2007;12:67–73.

25 Wen CY, Qin L, Lee KM et al. Grafted tendon healing in tibial tunnel is inferior to healing in femoral tunnel after anterior cruciate ligament reconstruction: A histomorphometric study in rabbits. Art Ther 2010;26:58–66.

26 Rodeo SA, Kawamura S, Kim HJ et al. Tendon healing in a bone tunnel differs at the tunnel entrance versus the tunnel exit: An effect of graft-tunnel motion? Am J Sports Med 2006;34:1790–1800.

27 Liu H, Fan H, Toh SL et al. A comparison of rabbit mesenchymal stem cells and anterior cruciate ligament fibroblasts responses on combined silk scaffolds. Biomaterials 2008;29:1443–1453.

28 Wen CY, Qin L, Lee KM et al. Peri-graft bone mass and connectivity as predictors for the strength of tendon-to-bone attachment after anterior cruciate ligament reconstruction. Bone 2009;45:545–552.

29 Tien YC, Chih TT, Lin JH et al. Augmentation of tendon-bone healing by the use of

calcium-phosphate cement. J Bone Joint Surg Br 2004;86:1072–1076.

30 Li YG, Wei JN, Lu J et al. Labeling and tracing of bone marrow mesenchymal stem cells for tendon-to-bone tunnel healing. Knee Surg Sports Traumatol Arthrosc 2011;19:2153–2158.

31 Ude CC, Sulaiman SB, Min-Hwei N et al. Cartilage regeneration by chondrogenic induced adult stem cells in osteoarthritic sheep model. Plos One 2014;9:e98770.

32 Hosseinkhani M, Mehrabani D, Karimfar MH et al. Tissue engineered scaffolds in regenerative medicine. World J Plast Surg 2014;3:3–7.

33 Fan H, Hu Y, Zhang C et al. Cartilage regeneration using mesenchymal stem cells and a PLGA-gelatin/chondroitin/hyaluronate hybrid scaffold. Biomaterials 2006;27:4573–4580.

34 Lui PP, Wong OT, Lee YW. Application of tendon-derived stem cell sheet for the promotion of graft healing in anterior cruciate ligament reconstruction. Am J Sports Med 2014;42:681–689.

35 See EY, Toh SL, Goh JC. Multilineage potential of bone-marrow-derived mesenchymal stem cell cell sheets: Implications for tissue engineering. Tissue Eng Part A 2010;16:1421–1431.

36 Guo S, Zhen Y, Wang A. Transplantation of bone mesenchymal stem cells promotes angiogenesis and improves neurological function after traumatic brain injury in mouse. Neuropsychiatr Dis Treat 2017;13:2757–2765.

37 Zhu F, Wang J, Qiu X et al. Smoke inhalation injury repaired by a bone marrow-derived mesenchymal stem cell paracrine mechanism: Angiogenesis involving the Notch signaling pathway. J Trauma Acute Care Surg 2015;78:565–572.

38 Liu SH, Panossian V, Al-Shaikh R et al. Morphology and matrix composition during early tendon to bone healing. Clin Orthop Relat Res 1997;339:253–260.

39 Schiavone PA, Fabbriciani C, Delcogliano A et al. Bone-ligament interaction in patellar tendon reconstruction of the ACL. Knee Surg Sports Traumatol Arthrosc 1993;1:4–8.

40 Lee CA, Meyer JV, Shilt JS et al. Allograft maturation in anterior cruciate ligament reconstruction. Art Ther 2004;20:46–49.

41 Goradia VK, Rochat MC, Kida M et al. Natural history of a hamstring tendon autograft used for anterior cruciate ligament reconstruction in a sheep model. Am J Sports Med 2000;28:40–46.

42 Cartmell JS, Dunn MG. Development of cell-seeded patellar tendon allografts for anterior cruciate ligament reconstruction. Tissue Eng 2004;10:1065–1075.

43 Kawamura S, Ying L, Kim HJ et al. Macrophages accumulate in the early phase of tendon-bone healing. J Orthop Res 2005;23:1425–1432.

44 Ditsios K, Boyer MI, Kusano N et al. Bone loss following tendon laceration, repair and passive mobilization. J Orthop Res 2003;21:990–996.

45 Mikos AG, McIntire LV, Anderson JM et al. Host response to tissue engineered devices. Adv Drug Deliv Rev 1998;33:111–139.

46 Basic-Jukic N, Ratkovic M, Radunovic D et al. Association of silicone breast implants and acute renal allograft rejection. Med Hypotheses 2019;123:81–82.

47 Krieger NR, Yin DP, Fathman CG. CD4+ but not CD8+ cells are essential for allorejection. J Exp Med 1996;184:2013–2018.

48 Mbiribindi B, Harden JT, Pena JK et al. Natural killer cells as modulators of alloimmune responses. Curr Opin Organ Transplant 2019;24:37–41.

49 Jitschin R, Mougiakakos D, Von Bahr L et al. Alterations in the cellular immune compartment of patients treated with third-party mesenchymal stromal cells following allogeneic hematopoietic stem cell transplantation. Stem Cells 2013;31:1715–1725. https://doi.org/10.1002/stem.1386.

50 Ankrum JA, Ong JF, Karp JM. Mesenchymal stem cells: Immune evasive, not immune privileged. Nat Biotechnol 2014;32:252–260.

51 Scheffler SU, Unterhauser FN, Weiler A. Graft remodeling and ligamentization after cruciate ligament reconstruction. Knee Surg Sports Traumatol Arthrosc 2008;16:834–842.